UNIVERSITÀ degli STUDI di CATANIA

DIPARTIMENTO DI INGEGNERIA ELETTRICA, ELETTRONICA E INFORMATICA

DOTTORATO DI RICERCA IN INGEGNERIA DEI SISTEMI, ENERGETICA, INFORMATICA E DELLE TELECOMUNICAZIONI
XXIX CICLO

Tesi di Dottorato

HYBRID MOBILE FEMTOCELLS

THE MMWAVE SOLUTION FOR 5G MOVING NETWORKS

ING. ANTONIO ROBERTO MASTROSIMONE

Coordinatore	Tutor
Chiar.mo Prof. P. ARENA	Chiar.ma Prof.ssa D. PANNO

ABSTRACT

Mobile connectivity is a vital requirement for people's everyday life. Users would like to have unlimited access to information for anyone, anywhere, and anytime, especially in public means of transport where they spend a lot of time travelling. The connectivity to Internet becomes difficult for passengers because public transportation vehicles suffer from the low quality signal from the outside wireless network.

One of the requirements of the 5G Network is to guarantee a high level of service to users wherever they are, both at home, office, or in public means of transport. Users on the move shall have the impression that "the network infrastructure follows them", especially in situations where they suffer from poor coverage today.

A first solution to improve the broadband connectivity is to deploy more eNodeBs close to buses or train routes, but it requires high investment for providers and a higher complexity in managing the increasing number of handover. The rapid growth in the deployment of LTE femtocells for indoor use and their benefits have led many authors to propose of using them even in vehicles, implementing the so-called Moving Networks. This work shows that the use of pure LTE mobile

femtocells exhibits relevant issues in terms of interference and consequently poor performance in a realistic use. In order to overcome these issues, we propose to adopt the millimeter Wave (mmWave) technology in the Moving Networks, creating the Hybrid Mobile Femtocells. The new technology will satisfy the 5G requirements of enhancing the capacity and coverage for the users on the move and to enable long battery life, due to the short range transmission between the user equipments and the access point.

In the thesis we discuss the concerns arising from applying mmWave communications at 60 GHz inside vehicles. We provide a new throughput analysis in order to benchmark our proposal to the solutions presented in literature. Furthermore, we analyse the system performance in two different scenarios: a sub-urban setup and in an urban configuration where different kind of cells are deployed. The results obtained by Matlab simulations, show a noticeable improvement of the global system throughput by using Hybrid Mobile Femtocells.

CONTENTS

CHAPTER

ONE

INTRODUCTION

1.1 Toward 5G

Mobile data traffic is growing faster than ever. Every year the demand in mobile broadband communications increases as more and more users subscribe to mobile broadband package. The amount of traffic has been doubling each year during the last few years with the increasing popularity of smartphones, super-phones and tablets with powerful multimedia capability and the necessity to reach data services and applications on mobile broadband [1, 2]. Global mobile data traffic grew 74% in 2015, 4000-fold over the past 10 years and almost 400-million-fold over the past 15 years. In the same year more than half a billion mobile devices and connections were added [3] and an astounding 1000-fold in data traffic is expected in this decade [4].

Long Term Evolution-Advanced (LTE-A) has been recently standardized by the Third Generation Partnership Project (3GPP), but

nevertheless industry and academia are working together to meet the capacity demand for mobile communication system. Several large scale project such as Mobile and wireless communications Enablers for Twenty-twenty Information Society (METIS) and 5GNOW have also recently started to investigate 5G mobile communication system, ranging from new radio access interfaces to new system architectures [5].

1.2 The METIS Project

METIS is an integrated project partly funded by the European Commission and is considered as the 5G flagship project [6]. It consists of 29 partners spanning telecommunication manufacturer, network operators, automotive industry, and academia that have the objective of founding the 5G mobile and wireless communication system.

5G network will have increased capacity, high data rate, low latency, reliability, scalability, flexibility [6, 7], and significant improvement in communications Quality of Service (QoS) in order to fulfil the growing demand for mobile connectivity (more than 50 billion devices are expected to be connected in 2020).

In particular, 5G should support:

- 1000 times higher mobile data volume per area;
- 10 to 100 times number of connected devices;
- 10 times longer battery life;
- 5 times reduced end-to-end latency.

METIS has analysed the above issues and it has defined five scenarios to target the right enabling technology components [6]:

- **Amazingly fast**: high data rates for future mobile broadband user experiences of instantaneous connectivity without delays. This enables the users to enjoy the work or infotainment with a instantaneous response perceived. The users will experience that they get all they need, when they need, wherever they will have the need [8]. The challenge is to provide high data rates at the application layer in order to encourage the cloud services and applications that users can access without any perceived waiting time.

- **Great service in a crowd**: 5G should solve the problem of denial of service for users located in very crowded area, such as stadium, open air festival, public events. Today, the experience of the users is compromised in crowded places, because the high number of mobile devices with a high density, causes an increase in network load. In the future the network will provide any kind of service even in very crowded places, despite the increase in traffic volume.

- **Best experience follows you**: the user's experience for end users should be the same at home, office, and on the move. Users shall have the impression that "the network infrastructure follows them", expecially in situation where they suffer from poor coverage today (e.g. in cars, busses, or trains). The goal is to ensure to end users a data rate of at least 100 Mbps in downlink and 20 Mbps in uplink with a end-to-end delay below

100 ms. It is required high robustness and ability to manage mobility with low battery consumption of end user terminals and at low cost.

- **Super real-time and reliable connection**: the future network will manage human users and machines that will autonomously communicate. New applications based on Machine-to-machine (M2M) communication with real time constraint (e.g. functionality for traffic safety and efficiency, mission-critical control for industrial applications), will require high reliability and low latency than todays communication systems: for certain use cases, a maximum End-to-End latency must be guaranteed with very high reliability, e.g. 99.999% [8].

- **Ubiquitous things communicating**: in the future, more and more new devices will be added in the network. The human centric communication will be joined to the machine-type communication. Simple and advanced devices will be connected and the network should be able to handle a large number of devices for different purposes.

1.2.1 The METIS Horizontal Topics

The challenges shown in the previous section will be addressed by a combination of different solutions. The METIS calls an overall system concept as "Horizontal Topics" (HTs) in its project. A HT is a scenario that integrates a subset of technology components to provide a solution for the requirements that the 5G mobile network will have to satisfy. The performance of each HT will be evaluated according to

the research objectives and KPIs and it has to ensure the integration of the developed technology components [6].

The highlights for the METIS HTs are given as follows:

- **Direct Device-to-Device (D2D) Communication**: it refers to the exchange of data among two devices without the intervention of the network that will control, under normal conditions, only the radio resource usage of the direct links in order to minimize the resulting interference. The introducing of D2D in 5G architecture will provide different benefits: increased coverage (availability and reliability), offload backhaul (cost efficiency), provide a fall-back solution (reliability), improve spectrum usage (spectrum efficiency), typical user data rate and capacity per area (capacity density), and enable highly reliable, low-latency Vehicle-to-Infrastructure (V2X) connections [9].

- **Massive Machine Communication (MMC)**: one of the requirements of the 5G is the scalability. The new network will be capable to support an unprecedented number of devices. The new radio access will include: direct access, for devices directly connected to the access node, access through accumulation/aggregation point, machine-type access for D2D communications. A large number of connected devices requires efficient techniques of resources allocation and mitigation of the interference issues.

- **Moving Networks (MNs)**: this topic introduces innovative directions for the future relationship between vehicles and wireless connections. The METIS defines three clusters:

    1. MN for mobility-robust high-data rate communication links

(MN-M), to enable broadband as well as real-time services in mobile terminals and moving relays;

2. MN for nomadic network nodes (MN-N), to enable a flexible and demand-driven network deployment;
3. MN for V2X communications (MN-V), to enable reliable and low-latency services such as road safety and traffic efficiency.

While the MN-M cluster represents an evolutionary improvement of the existent technology addressing highly mobile scenarios, the MN-N and MN-V clusters introduce a paradigm shift in the usage of mobile communications [9]. A MN consists of a node or a group of such nodes that communicates with its environment, that is, other nodes, fixed or mobile, inside or even outside the moving entity [6].

- **Ultra-Dense Networks (UDNs)**: in the near future, an ultra-dense deployment of small cells is expected. New spectrum flexible air interface will be used and new techniques such as resource allocation and coordination, auto-activation and deactivation of the cells, self-backhaul, need to be developed. A UDN will offer performance improvements in [9]:

  1. context awareness for mobility, resource and network management;
  2. inter-RAT/ inter-operator collaboration;
  3. tight interaction of a UDN layer with a macro layer holding superior role in control and management functions over common area;

4. macro-layer based wireless backhaul for flexible and low-cost UDN deployments.

- **Ultra-Reliable Communications (URC)**: one of the requirements of the 5G network is the reliability. The current operating mode of a mobile network will be changed. A URC will consist of spectrum allocation and management, robust PHY mechanisms, signalling structure and interface management, Multi-RAT, in order to respond to an objective: when the communication will be not available at a peak rate, the system will provide reliable moderate rates to all users instead of failing some of them. In this way, it will be guaranteed a minimum connectivity for the applications in case of emergency and for infrastructure damages.

- **Architecture (Arch)**: METIS researches and introduces new architectural concepts that will satisfy the 5G KPIs and requirements. The Radio Access Network will be dynamic and it will efficiently manage multiple layer and a variety of air interfaces both in access and backhaul links. The new architecture will be able to handle different QoS characteristics, such as ultra low latency traffic, ultra reliable communications, broadcast traffic etc. The requirements of scalability and flexibility will be reached by using the new technologies in terms of Software Defined Network (SDN), Self-Organized Network (SON), Network Functions Virtualization (NFV).

To solve the aforementioned challenges, it becomes essential to adopt a network infrastructure that can efficiently integrate various

wireless technologies and to enable inter-networking of existing and newly-deployed technologies [10]. 5G will realise networks capable of providing zero-distance connectivity between people and connected machines in a truly connected society with unlimited access of information for anyone, anywhere, and anytime [11]. In order to fulfil these requirements, 5G network should adopt a heterogeneous architecture with different kinds of cells (macrocells, small cells, and relay nodes) [12], multiple radio access technologies (RATs), massive Multiple Input Multiple Output (MIMO) at Base Stations (BSs) and/or user equipments (UEs) that will support microwaves and mmWave frequency bands [10].

1.3 Motivation and basic idea

1.3.1 Vehicular users issues

It has been shown that a significant number of users accessing wireless broadband services while riding vehicles and this number is increasing significantly because of the high penetration of UEs. Users are expecting similar experience at home, in the office, when stationery or travelling. In literature, a group of users who accessing the mobile network from inside the vehicle, is known as **Vehicular Users (VUEs)**. A significant attention has been paid to address the issues of the VUEs because they suffer from low signal quality caused by the poor macro antenna coverage of base stations inside vehicles with metallic walls [13].

The Vehicular Penetration Loss (VPL) is one of the biggest factors that limit the performance for VUEs. According to [14], the measured

VPL can be as high as 25 dB in a minivan at the frequency of 2.4 GHz, and higher VPLs are foreseeable in higher frequency bands.

Hence, the communication "on the move" exhibits a low throughput for users and a greater energy consumption. The problem becomes more critical for users that access the mobile network on public transportation vehicles (e.g. trains, buses, or trams, etc.). In this case many users in a single moving vehicle simultaneously perform network operations such as multiple individual handovers. As a result, the network must be able to manage numerous real-time handover procedures requiring more resources, signalling overhead and reporting delays.

1.3.2 Moving Networks Solutions

Both 3GPP and METIS have taken the issues of the vehicular users into account. The first proposes various solutions within the Heterogeneous Network deployment in order to increase the vehicular users performance. The latter addresses the issues in one of the HT, the "Moving Networks" (MNs) that enhance and extend the coverage for many communication devices that move together.

So far, the most promising solution for the MN scenario, seems to be the combination of the concepts of mobile relay and femtocell, the so called Mobile Femtocell Architecture.

1.3.3 Mobile Femtocell Architecture

Several studies in literature showed that the use of the Femtocell Access Point (FAP) improves the users throughput and extends the network coverage in indoor environment [15, 16, 17].

Femtocell concept has found a place in the architecture of LTE networks as a cost–effective solution designed to improve both coverage and user throughput in residential and enterprise environments (where mobile users spend most of time), as well as to offload data traffic from macrocell network.

Femtocells, also called Home eNodeB (HeNB), are low–power, short–range, plug–and–play cellular Base Stations (BSs) that operate in a licensed spectrum. FAPs are conceived to be installed by end consumers in ad–hoc manner, rather than being part of a planned deployment, and are connected to the operator core network via the user's existing broadband Internet access (e.g. digital subscriber line or coaxial cable). Femtocells are equipped with omnidirectional antennas with a transmit power of about 100 mW and provide a coverage of about 20 m.

The benefits arising from the use of FAP are manifold:

- **Improved coverage and capacity**: the short distance between serving cell and users provides high data rates and improves data reception even when there is no existing macrocell signal or it is poor.
- **Cost benefits**: the operator can extend and improve coverage with low operating and capital costs, as deployment of FAPs will reduce the need for adding macro base stations.
- **Improved battery life**: the mobile phones benefit of an energy saving in transmission due to the short distance between transmitter and receiver.

Due to the simple installation and the many advantages, a large dif-

fusion of LTE femtocell devices in residential and enterprise environments is expected in the near future.

For these reasons, many authors [13, 18, 19, 20, 21] suggest that the FAP can be a natural opportunity for vehicular environment in order to realise a practical implementation of the **"Mobile Femtocell"** [18] as a new Moving Network (MN) architecture in LTE environment.

Mobile Femtocell Access Point (MFAP) is located inside a vehicle and use two antennas. The users inside the vehicle communicate with the MFAP through an omnidirectional indoor antenna, while a large array antenna is located outside the vehicle and permits the MFAP to communicate with the eNodeB. Consequently the vehicular penetration loss can be reduced. Furthermore, the outdoor array antenna has a gain that strengthens its received signal.

1.3.4 Hybrid Mobile Femtocells

The use of Mobile Femtocells that work in the same LTE band of the macrocells can suffer from severe QoS degradation, because of the inter-cell interference that can arise between fixed and moving cells [22, 23]. So, in according to the METIS vision that suggests to use new frequency bands in 5G system [10] to increase the system capacity, we propose to adopt the mmWave technology for the in-vehicle communications, creating the **Hybrid Mobile Femtocells** that use both mmWave and LTE band in order to reduce the interference issues. mmWaves are currently been used for high speed Line of Sight (LOS) links and they are considered as the main technology for the next-generation mobile communication systems [24, 25].

The benefits of applying the mmWave approach in in-vehicle link

between users and the MFAP, are as follows:

- users inside the public vehicles will take advantage of strong short range signal transmitted by the MFAP;
- some interference issues will be solved because the nodes will use different frequency bands;
- greater throughput will be available to vehicular and macrocell users.

In this thesis, we investigate if the adoption of Hybrid-Mobile Femtocell Access Point (H-MFAP) can be really considered an effective and viable solution to the future MN. The feasibility of the solution is analysed by benchmarking H-MFAP with the other solutions presented in literature. The performance analysis include the propagation model and the evaluation of the SINR measured by the user equipments. A new throughput model is presented for evaluating the use of H-MFAP in different configurations, suitable for sub-urban and urban scenario.

1.4 Structure of this Dissertation

The thesis is organised as follows. In Chapter 2 we discuss about the different implementations of a Moving Network (MN) addressed in literature. The issues of Mobile Femtocells that use LTE technology are discussed in Chapter 3. The Millimeter Wave characteristics and applications are presented in Chapter 4. Our proposal is presented in Chapter 5. Chapter 6 describes the system models adopted for sub-urban and urban scenarios. In order to compare several MFAP

solutions a new throughput model is introduced in Chapter 7. The simulation results and the case studies are shown in Chapter 8. Finally, Chapter 9 concludes this dissertation.

1.5 Acknowledgement

First of all, I would to thank my supervisor, Prof. Daniela Panno, for the support, advices and for being always ready to help. Under her guidance and patience it was possible to get this achievement.

I sincerely thank all the professors and the staff of the DIEEI who have always supported me during these years.

Then I want to thank my family that always believe in me, and my nephews, that although distant, give me the joy of going forward.

CHAPTER

TWO

LITERATURE OVERVIEW

Different types of low power cells (pico eNodeB, remote radio heads, fixed relay nodes, moving relay nodes, home eNodeB) deployed under the coverage of macro eNodeBs constitute a Heterogeneous Network (HetNet) with the aim to meet the capacity need in specific hot spot area [26]. This architecture is widely considered in 5G standardization, in particular for supporting a very dense deployments of wireless communication links in urban environments, where the small cells can meet the capacity needs in specific hot spot area while the macrocells provide basic coverage.

2.1 3GPP solutions

HetNet deployment is recommended by 3GPP that propose in [27] different solutions of this architecture in order to increase the performance of the VUEs. Lets analyse them in detail:

- **Dedicated deployment of macro eNodeB**

  When the route of a public transportation vehicle is known, the coverage of macro base stations can be enhanced by deploying dedicated eNodeBs with directive antennas, along the trains lines or highways. To reduce UE handover failure rate, to extend coverage and capacity, and to reduce costs, a HetNet deployment can be used in this scenario with the use of high-power cells (eNodeB) and fixed low-power cells. The eNodeBs can be configured as the serving node, while low power nodes provide high data rates. It is necessary to coordinate the operations of the cells. Different approaches could be possible, such as Carrier Aggregation (CA), in which the high power cells transmit the Primary Component Carrier (PCC) while the Secondary Component Carrier (SCC) is transmitted by the low-power nodes, or by using cross-carrier scheduling schemes. However, the VPL remains an issue because it cant be reduced in this solution due to the presence of outdoor fixed access points. Moreover site acquisition, deployment, maintenance are a challenge for operators especially in urban scenarios [21].

- **Dedicated deployment of macro eNodeB + L1 repeaters**

  Layer 1 repeaters amplify and forward signals in a certain frequency band. In a public transportation vehicle if the RX and TX antennas are well isolated (i.e. inside vs. outside the vehicle), the repeaters can work in full-duplex mode, by using the same frequency band inside and outside the vehicle. In this way the VPL can be reduced, and the VUE can transmit data with lower power. Since the repeaters do not re-generate the received

signal, the SINR cannot be improved because the L1 repeaters amplify both noise and desired signal. Moreover the core network does not control them, so the handover of the VUEs will be performed individually. In dense deployment scenarios, the L1 repeaters may bring more interference into the system [21].

- **LTE as backhaul, Wi-Fi as Access on Board**

  Nowadays, the use of WiFi Access Point on board is highly popular. It consists of a WiFi hotspot that uses LTE for backhaul. All VUEs can use this node only for data connections or VOIP calls, while continuing to use the cellular network for voice calls. VPL can be avoided, group handover can be used, but only for data traffic. This solution also enables any Wifi-only devices to use LTE network as backhaul, but without authentication, security and QOS support offered by the core network. Moreover, as the WiFi operates on the open industrial, scientific and medical radio (ISM) bands, the interference issues cannot be coordinated [21].

2.2 Mobile Relay Node deployment

The Mobile Relay Nodes (MRNs) are base stations/access point mounted on vehicles. They use two antennas: one outside the vehicle, used for the connection to the Donor eNodeB (DeNB) via LTE Un radio interface, while the users inside the vehicle communicate with them through an omnidirectional indoor antenna. MRN may support multi-RAT functionalities, so VUEs can be connected to it through different air interface technology, e.g. LTE/3G/2G. Authors in [18]

propose to communicate via LTE in both link (to the DeNB and to VUEs), so they combine the concepts of relay node and femtocells as an implementation of MRN in a so called **Mobile Femtocell Access Point (MFAP)** architecture. It provides eNodeB functionality and supports a subset of the UE functionality to connect to the DeNB. Using MFAPs, vehicular users may obtain high coverage and more system capacity. MFAP provides uninterrupted connectivity for the user plane and control plane of the served UEs, moreover, the drop calls and the signal overhead are reduced because the MFAP creates its own cells within a vehicle. So, it and its associated users are viewed as a single unit by the eNodeB that can perform a single group handover for all users connected to it [28]. A further advantage is the energy saving on UE: battery life can be extended thanks to shorter communication range with MFAP. Moreover, the outdoor array antenna has a moderate gain that strengthens its received signal. Consequently the VPL can be eliminated with a reduction of the outdoor-to-indoor signal strength.

To the best of our knowledge, all existing studies related to MN apply MRN architecture in LTE systems.

Authors have dealt with different aspects of this architecture. Let's analyse them in detail:

2.2.1 Coverage and spectral efficiency

In [19, 20, 21, 29, 30] the potential advantages of the use of LTE-based MFAP in vehicular environment in terms of coverage and spectral efficiency have been investigated.

In particular, authors in [19] compare the capacity obtained consid-

ering three modes: a traditional mode, a pure relay mode, a femto-like mode. In the first schema there are not mobile relay, in the second they introduce a resource allocation by means a time division model: when the mobile relay transmits to its users, the eNodeB stops the communications to ordinary users. In the third mode they propose to use a MFAP that re-use the frequency of the macrocell. The paper shows that femto-like mode can bring almost +100% the capacity gain compared to traditional mode thanks to the frequency re-use and the high penetration loss of the bus. The effects of the transmission of the MFAP to the macrocell users are not taken into account.

Also authors in [20] calculate the capacity and the outage probability obtained in a system with the presence of MFAPs. Their simulation results demonstrate that the MFAPs can improve the performance of vehicular users, but in their model, the MFAPs use different frequency of the macrocell and the interference from other femtocells is not considered.

In [21] authors explore the different solutions used to solve the vehicular issues and a deep analysis of the MRN comprising challenges and open issues.

In [29] authors show the performance of fixed and mobile femtocells and the improvements obtained under a condition: they should be deployed at macrocell cell edge in order to reduce the interference caused by the proximity of the eNodeB.

In [30] the objective is to compare the differences between the relaying network architecture with mobile or fixed relay station. Authors show the different advantages and disadvantages for each relay station method and then compare the performance by measuring the capacity gain. Their simulation results show that the fixed relay nodes

(FRS) deployed in an urban scenario outperforms the mobile relay architecture (MRS). However, only if the deployment of the FRS is cost efficient, it is reasonable to think that relaying will be first performed through FRS. Otherwise, another alternative would be to use vehicles as relay station.

2.2.2 Handover procedures

In high speed Moving Network there is the problem of the frequent handover procedures that may occur. In [31, 32] the authors propose solutions for handover procedures in the Mobile Femtocell Networks.

In [31] a new handover scheme is proposed in order to guarantee the seamless connectivity and to improve the QoS for high speed moving vehicular femtocell networks. The performance of the algorithm is evaluated by measuring the SINR and outage probability.

In [32] authors propose a resource management scheme that contains bandwidth adaption policy and dynamic bandwidth reservation policy in order to manage different scenarios of group handover. They propose a schema that improve the performance of the handover when the bus arrives at the station and a number of users get off form the vehicle and execute multiple handover from the FAP to the macrocell and vice versa. Moreover, when the vehicle is in movement, only its outsider receiver executes handover between the backhaul networks, since the MFAP and its associated users are viewed as single entity. So, it is necessary that the macrocell has sufficient resources and bandwidth to allow the procedure.

2.2.3 Interference issues

Authors in [13, 18, 33] focus on the problems of interference and propose different resource allocation schemes. The resource allocation is itself a challenging problem in cellular networks. For achieving high system throughput, it is necessary to satisfy two dual conditions: maximizing the spectral efficiency and minimize interference. If finding a good compromise between these two opposing requirements is already difficult in the case of fixed femtocells, it would be more challenging for mobile femtocells to maintain high network performance. Authors [18, 19, 20, 21] suggest that higher performance can be obtained by re-using the macrocell frequency band in the MFAP coverage area. In this way a higher spectral efficiency could be obtained, but it must handle the channel interference issues caused by the use of the same resources. This problem is expected to become more significant in the near future due to the large deployment of fixed and mobile small cells. Reusing the same bands within the small cells and concurrently handling interference problem are dramatically difficult, especially with moving cells.

CHAPTER

THREE

ISSUES ON LTE-MFAP

In the following we consider a macrocell with public busses equipped with MFAP devices. We specify two kinds of mobile users: out_UE, user equipment outside the vehicles and served by the eNodeB; VUE, user equipment inside the vehicles. According to 3GPP convention, the MFAP system distinguishes three kinds of links (Fig. 3.1): "backhaul link", the link between the DeNB and MFAP; "access link", the link between the MFAP and the VUE; "direct link", the link between the eNodeB and the out_UE.

For a pure LTE MFAP (L-MFAP), the backhaul and access links are based on LTE radio access. We focus on downlink communications. The MFAP decodes and buffers data received from the backhaul link and then forwards them to the VUEs. These two phases cant be done at the same time. In order to reduce the interference that may arise between the transmissions on access and backhaul links, a time division scheme for these two transmissions can be adopted as an easier

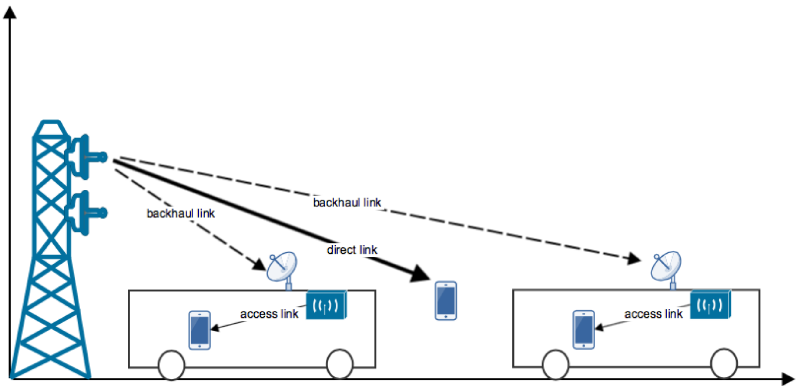

Figure 3.1: *MFAP architecture with the different names of the links*

and a more natural solution.

At this regard, [18, 19] propose the use of a time interval for the simultaneous transmissions on the backhaul and direct links, and another interval for transmission on the access and direct links. In the first interval, due to the fact that the MFAP is seen as an *out_UE* from the eNodeB and the orthogonal nature of OFDMA, there is no interference between backhaul and direct links. In the second interval, due to the simultaneous transmissions by two nodes (eNodeB and MFAP), appropriate resources allocation policies are required. In [18], two resource partitioning schemes are investigated:

- an **orthogonal partitioning scheme** in which the whole system bandwidth is divided in two different sub-bands, one for each node;

- a **non-orthogonal scheme** in which the whole bandwidth can be simultaneously used by both nodes.

In the first scheme there is no interference, but it has the drawback of a poor spectral efficiency due to the subset of orthogonal frequencies that can be used. For this reason, the orthogonal partitioning scheme appears to be anachronistic in a 5G system where more and more capacity is required. In the second scheme, the out_UEs and $VUEs$ use the same LTE bandwidth and the same technology. In this way the resource utilisation is improved and the Radio Resource Management is more flexible than the first scheme. However, it introduces intra-cell interference between the users of access and direct links. The aim of the thesis is to evaluate how these interference issues affect the performance of the system in different scenarios. We will show that the interference caused by the direct link transmission on the access link, is negligible when the MFAP moves away from the eNodeB site. In this case, since the eNodeB signal strength is poor, the metal walls of public transport means insulate it from external transmissions. Conversely, the interference caused by the access link transmissions on the direct link is always remarkable.

These restrictions become burdensome in a real-scenario where the MFAP moves around a city. In literature [18, 20, 29, 33], the use of L-MFAPs is recommended only in half and edge of the cell. In particular, when the bus is approaching the eNodeB site, $VUEs$ served by the L-MFAP measure a low SINR. So, in [18], it is suggested that they will be forced to disconnect from L-MFAP and to switch to eNodeB. Unfortunately this results in a high number of simultaneous handovers. Moreover, as the bus moves, as soon as the signal of the MFAP becomes acceptable, users will have to re-engage with the MFAP causing additional handover procedures.

Analogously, in [29] the authors suggest that out_UEs, far away

from their serving eNodeB and in proximity of a bus, could trigger a handover toward MFAP. However, because this connection is active only for a short time, depending on the speed of the bus, this event can determine QoS degradation and call dropping.

In conclusion the solutions proposed so far in the literature exhibit a high performance only in limited scenarios. They do not take into account that in real operating conditions, the system could suffer from severe QoS degradation in terms of global throughput and/or signalling load.

CHAPTER

FOUR

MILLIMETER WAVE TECHNOLOGY

The continuous increase of speed and bandwidth requirements have meant that the scientific community moves its interest toward the electromagnetic spectrum that extends between 30 and 300 GHz, which corresponds to wavelengths from 10 to 1 mm. Although the mmWave technology has been known for several years, it was preferentially used for military purposes, satellite, and point-to-point communications. The advances in technology and the low cost integrated solutions have meant that this frequency band take a major consideration to both academia and standardisation groups.

Most of the current research is focused on the 28, 38, 60 GHz band, and the E-band (71-76 and 81-86 GHz). Both industry and academia are working for standardisation activities in wireless area network, such as IEEE 802.15.3 Task Group 3c (TG3c) [34], IEEE 802.11ad standardisation task group [35], Wireless HD Consortium, Wireless Gigabit Alliance (WiGig) [24]. There are several ongoing discussions

within research projects such as FP7 EU Project METIS [6] on how to incorporate mmWave network in 5G [36]: the potential applications include small cell access, cellular access and wireless backhaul [37].

4.1 mmWave characteristics

There are many differences between the mmWave communications and the microwaves bands, so there are many challenges in physical, medium access control and routing layers due to two main aspects: the free space propagation and loss factors.

4.1.1 Free space propagation

As all the spherical waves, the transmitting power scales with the square of link distance and carrier frequency. This effect is due to the spherical spreading of the radio waves as they propagate, so, when the distance between a transmitter and a receiver antenna is doubled, the power received is reduced by a factor of four.

The free-space loss between two isotropic antennas at a distance R can be expressed by the following formula:

$$L = 20 \cdot log_{10} \left(\frac{4\pi R f}{c} \right) \tag{4.1}$$

where c is the light speed in vacuum ($\simeq 3 \cdot 10^8\, m/s^2$), f the frequency considered expressed in Hz, R the distance between the two antennas in m.

In (4.1) we can note that the free space loss considerably increases when the work frequency is higher. So, considering a signal at 60

GHz, the signal power has an attenuation of almost 36 dB higher than a signal at 1 GHz. For this reason, it is suggested to use the mmWave for short range communication link.

4.1.2 Atmospheric losses factors

There are also physical aspects of the radio propagation channel that require particularly attention at this frequency band. It occurs to consider the attenuation effects due to the rain drop, water vapour and oxygen.

The gaseous attenuation depends on the pressure of the gas, the temperature, and the density. These losses are greater at the frequencies that coinciding with the mechanical resonant frequencies of the gas molecules. Water vapour exhibits three absorption peaks at 22, 183, 323 GHz that are shown in Fig. 4.1 [38] by considering an atmospheric pressure of 1 atm, a temperature of $20 \circ C$, and a water vapour density equals to $7.5 g/m^3$ at sea level. To avoid losses, it is necessary to do not use the frequencies that correspond to the peaks. Fig. 4.1 also shows the oxygen absorption that exhibits two peaks at 119 GHz (1.7 dB/Km) and at 60 GHz where the attenuation value is the highest (15.5 dB/Km), but the losses due to water vapour can be neglected (0.1 dB/Km).

Let's note that the attenuation factors depend on the distance between the two antennas, so these mechanisms become relevant for mmWave links exceeding 100 m and crucial for longer distance like 1 km [39]. For these reasons, authors in [24, 25] suggest to use mmWave in indoor scenarios where they propose to use the same modulation schemes of 4G LTE Network (OFDMA and SC-FDMA).

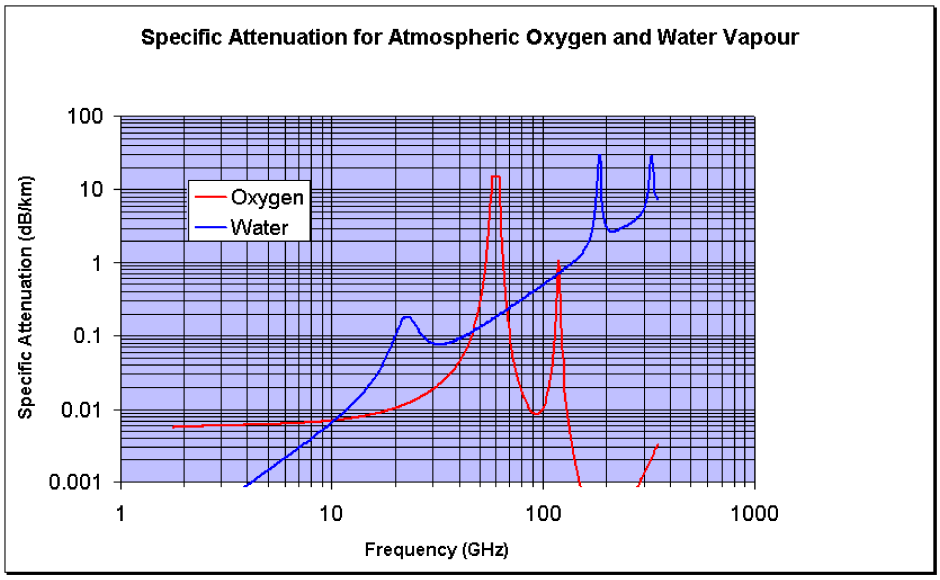

Figure 4.1: *Specific attenuation for atmospheric oxygen and water vapour [38]*

Although it might seem like an inconsistency, for micro and pico-cellular applications, where the cell radius does not exceed 1 km and 100 m respectively, it is preferable to use a set of frequencies around the 60 GHz, where the major attenuation is due to the oxygen. In fact, in these contexts, the oxygen attenuation increases, in a natural way, the separation between co-channel cells. As a result, the frequency reuse factor can be reduced.

4.1.3 Rain attenuation

It also occurs to considerate the attenuation due to the rain. By considering a frequency of 60 GHz, the interaction between the raindrop and the electromagnetic waves, creates an attenuation that depends on the size and shape of the raindrop. Authors in [40] analyse the rain attenuation at 60 GHz and, considering a rainfall rate of 50 mm/h, the attenuation equals to 18, 14, and 8 dB/Km in according to the distributions of Person (LP), Lognormal (LN), and Best (BE), respectively.

It is important, for establishing a new radio link in outdoor environment, to know the statistics of the rainfall rate in the region of interests.

4.1.4 Scintillation fading

The scintillation fading is a phenomenon that affects the electromagnetic waves during their propagation and induces fluctuations of the received signal in amplitude and phase. It is due to the random fluctuations of the refraction index caused by the tropospheric turbulence.

Experimental measurements show that the scintillation effect can be neglected in practical application of the mmWave [40].

4.2 Advantages and applications

There are several advantages using the 60 GHz bands: highly secure operations thanks to the short transmitting range, high-speed links (wireless fiber), high level of frequency re-use enabled, mature technology (this spectrum has a long history of being used for secure communications), carrier-class communication links enabled with 99.999% of availability [41], large bandwidth available (from 56 GHz to 66 GHz in Europe). If we consider Shannons capacity formula, the sheer capacity of a mmWave system is enormous. As a result, large band interval per channel can be allocated (e.g. 220 MHz or more compared with 5-20 MHz in todays microwave system [24]).

New design guidelines are proposed for this technology: the small wavelength at 60 GHz frequency makes it possible to pack a large number of antennas into small size and low power transceivers, where the use of the MIMO techniques can enhance spectral efficiency [42].

Large companies, such as Samsung, are already developing new multiband smartphones that will also allow access to the LTE and mmWave [43] technologies.

CHAPTER

FIVE

OUR PROPOSAL: HYBRID-MFAP

In order to guarantee the use of MFAP as Moving Network in all conditions, regardless of the proximity to the eNodeB or other MFAPs, we have thought to use the mmWave technology in the access link.

We propose a new MRN architecture that uses LTE technology to communicate with eNodeB in the backhaul link, and to adopt mmWave inside the vehicle for the access link.

Hybrid-MFAP (H-MFAP) is the name of our new concept of MFAP for a MRN implementation. However, several aspects need to be examined so the use of H-MFAP can be really considered an effective and viable solution. What frequency band is more suitable? Is it available? Is the technology ready? Are the performance as we expect?

By considering that $VUEs$ are in a kind of indoor environment with short range links, we propose to use 60 GHz-mmWave in the access link of a H-MFAP. In this way, thanks to the addition of the

new frequency band, we solve the interference problems with other technologies that uses LTE.

The benefits of applying the mmWave approach in in-vehicle link between users and the MFAP, are as follows:

- users inside the public vehicles will take advantage of strong short range signal transmitted by the MFAP;
- some interference issues will be solved because the nodes will use different frequency bands;
- greater throughput will be available to vehicular and macrocell users.

However, we also must verify, for example, if the interference issues between nearby H-MFAPs arise and if the performance of the H-MFAP are significant in order to justify the introduction of this architecture.

CHAPTER

SIX

SYSTEM MODEL

In the following sections, we want to analyse the performance achievable with the adoption of mmWave-based MFAP (H-MFAP) compared to those exhibited by L-MFAP. In order to carry out a more thorough investigation, we consider two significantly different configurations of cells deployment for Sub-urban and Urban scenarios. In both scenarios we make the following assumptions:

- the H-MFAPs use a dual mode technology, mmWaves for the access link and LTE for the backhaul link;
- for the mmWave radio access in H-MFAP, we consider a carrier of 60 GHz and a bandwidth of 220 MHz as in [22];
- the UEs are equipped with transceiver of multi-standard technologies (e.g. mmWave and LTE). When a UE gets on a bus equipped with H-MFAP, it performs a handover procedure to the mmWave technology.

In the *"Sub-urban"* Scenario the area is covered by contiguous macrocells where we consider that:

- the access and the backhaul link use the same LTE band with a carrier at 2.6 GHz;
- any MFAP in the backhaul link communicates to DeNB by means LTE Resource Blocks (RBs) with a carrier of 2.6 GHz and this link has an Antenna Gain over the direct link;
- the L-MFAP deployed in a bus can operate in non-orthogonal or orthogonal allocation schemes;
- there are a number of out_UEs in a macrocell area served by the eNodeB by means of a direct link in LTE at 2.6 GHz.

In an *"Urban"* Scenario, in order to fulfil the requirements of capacity and coverage, a dense deployment of small cells embedded in a macrocell will be necessary. Due to the dense deployment of HetNet in this context, in order to reduce the inter-cell interference, we consider, as in [5], that small cells (femtocells and picocells) coexist and work in the same LTE bandwidth (2.6 GHz band), while the eNodeB of the macrocell transmits in the 800 MHz band. In this topology, we assume that:

- any MFAP communicates with the DeNB by means of a backhaul link at 800 MHz;
- the access link of L-MFAP uses the LTE technology with a carrier of 2.6 GHz;

- in the macrocell area there are a number of UEs connected to the picocells (pico_UEs) that work at 2.6 GHz.

CHAPTER

SEVEN

PERFORMANCE ANALYSIS

7.1 Propagation Models

For each link we consider an opportune propagation model as suggested in literature. In each one, d is the distance between the UE and its serving access point (eNodeB, MFAP or pico base station) of the path loss. Log-normal shadowing (S) is applied to all link with different standard deviation values. According to the ITU-R we used $S(\sigma_1)$ for the standard deviation of shadowing in sub-urban macro cell area (SMa), $S(\sigma_2)$ for the access link by considering the standard deviation for ITU-R Indoor Hotspot (InH) in LOS conditions, while $S(\sigma_3)$ is the value used for mmWave link [44]. The values are shown in Table 8.1.

The UEs connected with the eNodeB, e.g. direct links, are considered in the outdoor sub-urban environment. So, the propagation

model can be modelled as follows [44]:

$$L_{direct}(d) = 15.3 + 37.6log_{10}(d) + S(\sigma_1)\ [dB] \tag{7.1}$$

For the backhaul link, the path loss model used is the same of the direct link (7.1) considering also the Antenna Gain (Ag):

$$L_{backhaul}(d) = 15.3 + 37.6log_{10}(d) - Ag + S(\sigma_1)\ [dB] \tag{7.2}$$

The LTE access link is modelled with a model as in [31]:

$$L_{access}(d) = 20log_{10}(f_{MHz}) + 28log_{10}(d) - 28 + S(\sigma_2)\ [dB] \tag{7.3}$$

where f_{MHz} is the LTE carrier frequency.

For the access link in mmWave technology we consider the propagation model as in [45]:

$$L_{mmWave}(d) = PL_0 + 10 \cdot \alpha \cdot log_{10}(d) + S(\sigma_3)\ [dB] \tag{7.4}$$

where PL_0 is the free space Path Loss at 1 m (68 dB at 60 GHz), α is the exponential factor, equals 2.17 for a Line-of-Sight indoor hall.

In an urban scenario, we consider the presence of the picocell base stations. The link between the $pico\_UEs$ and its serving cell, is modelled as in [44]:

$$L_{pico}(d) = 30.6 + 36.7log_{10}(d) + S(\sigma_4)\ [dB] \tag{7.5}$$

where Log-normal shadowing effect is modelled by considering a standard deviation of the ITU-R urban microcell (UMi) model, $S(\sigma_4)$.

7.2 SINR Calculation

For each UE we estimate the SINR as the ratio between the signal power received from its serving Cell (Macrocell, Femtocell, Picocell), and the total interference power due to the co-channel transmissions plus the Thermal Noise (N).

In the following formulas, Lw_1 and Lw_2 are the attenuation experienced by signals entering the vehicle when LTE or 60 GHz link are considered, respectively.

For convenience, we use the following notation $SINR_y^x$ to indicate the SINR measured in the link y (y may assume the values D, A, B, that stand for: **D**irect, **A**ccess, **B**ackhaul) using the solution x (x may assume the values W, O, N, H, that stand for: **W**ithout MFAP; L-MFAP with **O**rthogonal allocation scheme; L-MFAP with **N**on-orthogonal allocation scheme; **H**-MFAP). Let's note that in some cases the interference is zero, but we maintain the same notation (SINR) for homogeneity.

The SINR measured by the MFAP in the backhaul link is equal to:

$$SINR_B = \frac{P_1 \cdot L_{backhaul}(d_{j,e})}{N} \tag{7.6}$$

where P_1 is the transmission power of the eNodeB, $d_{j,e}$ is the distance in meters between the MFAP j and the donor eNodeB e. Please note that we do not have interference because we are considering a single macrocell where the MFAP is viewed as an out_UE by the eNodeB, so it has been assigned orthogonal resources like the other UEs.

The SINR measured by a VUE without MFAP is calculated as

follows:

$$SINR_e^W = \frac{P_1 \cdot L_{direct}(d_{m,e}) \cdot Lw_1}{N} \tag{7.7}$$

where, $d_{m,e}$ is the distance in meters between the eNodeB e and the UE m. Again, we have not to considerate any interference because in a single macrocell scenario, all the UEs have orthogonal resources assigned by the OFDMA mechanism.

7.2.1 Calculation of SINR when the access link operates in LTE mode with Orthogonal allocation scheme

The L-MFAP that operates in orthogonal allocation scheme does not suffer from the interference issues due to the frequency band reuse. So, for an out_UE, the SINR in direct link is calculated as:

$$SINR_D^O = \frac{P_1 \cdot L_{direct}(d_{n,e})}{N} \tag{7.8}$$

where $d_{n,e}$ is the distance in meters between the eNodeB e and the out_UE n.

The SINR for a VUE served by the L-MFAP k, is calculate as follows:

$$SINR_A^O = \frac{P_2 \cdot L_{access}(d_{m,k})}{N} \tag{7.9}$$

where P_2 is the transmission power of the L-MFAP; $d_{m,k}$ is the distance in meters between the VUE m and the L-MFAP k.

7.2.2 Calculation of SINR when the access link operates in LTE mode with Non-orthogonal allocation scheme

In the cases of the L-MFAP that operates in Non-orthogonal allocation scheme, it re-uses the same bandwidth of the macrocell, so it is necessary to considerate the interference contributions of the transmission of the neighbouring MFAP and eNodeB.

The SINR of the direct link for an $out\_UE\ n$, is given by:

$$SINR_D^N = \frac{P_1 \cdot L_{direct}(d_{n,e})}{I_f + N} \tag{7.10}$$

In (7.10) the interference (I_f) due to the J neighboring L-MFAPs is:

$$I_f = \sum_{j=1}^{J} P_2 \cdot L_{access}(d_{n,j}) \cdot Lw_1 \tag{7.11}$$

where $d_{n,j}$ is the distance in meters between the $out\_UE\ n$ and the L-MFAP j.

In the access link, the $VUE\ m$, served by a L-MFAP k, measures a SINR equals to:

$$SINR_A^N = \frac{P_2 \cdot L_{access}(d_{m,k})}{\sum_{j=1,j\neq k}^{J}(P_2 \cdot L_{access}(d_{m,j}) \cdot 2 \cdot Lw_1) + I_M + N} \tag{7.12}$$

In (7.12) we consider the interference power I_f of the J-1 neighbouring L-MFAP, each at a distance of $d_{m,j}$ meters from the $VUE\ m$, and two penetration loss factors due to the presence of two walls of

the neighboring buses; I_M is the interference power received from the eNodeB e given by :

$$I_M = P_1 \cdot L_{direct}(d_{m,e}) \cdot Lw_1 \tag{7.13}$$

7.2.3 Calculation of SINR when the access link operates in mmWave technology

Due to the different frequency bands used in this case, the UEs connected to the eNodeB do not suffer from the interference of the H-MFAP transmissions. The $out\_UE\ n$ in the direct link, measures a SINR level equal to:

$$SINR_D^H = \frac{P_1 \cdot L_{direct}(d_{n,e})}{N} \tag{7.14}$$

In the access link, we have to consider only the inter-H-MFAP interference, so the SINR for a $VUE\ m$ is:

$$SINR_A^H = \frac{P_2 \cdot L_{mmWave}(d_{m,j})}{\sum_{j=1,j\neq k}^{J}(P_2 \cdot L_{mmWave}(d_{m,j}) \cdot 2 \cdot Lw_2) + N} \tag{7.15}$$

where P_2 is the transmitting power of a H-MFAP in mmWave technology.

7.2.4 Calculation of SINR of the UE connected to a pico base station

In an urban scenario with a dense deployment of small cells, both L-MFAP and picocell use the sameLTE frequency band at 2.6 GHz,

while the eNodeB of the macrocell transmits data in different band (800 MHz). We evaluate the SINR of the *pico_UEs* as follows:

$$SINR_{pico\_UE} = \frac{P_3 \cdot L_{pico}(d_s)}{I_{MFAP} + I_p + N} \tag{7.16}$$

where P_3 is the transmitting power of a pico base station, d_s the distance between a *pico_UE* and its serving pico base station; I_{MFAP} and I_p are the interference contributions of the nearby MFAPs and picocells respectively. In particular,

$$I_{MFAP} = \sum_{j=1}^{J} P_2 \cdot L_{pico}(d_j) \cdot Lw_1 \tag{7.17a}$$

where d_j is the distance between the *pico_UE* and the interfering L-MFAP j with non-orthogonal allocation scheme;

$$I_{MFAP} = 0 \tag{7.17b}$$

in the case of vehicles equipped with H-MFAP.

7.3 A new Throughput Model

In the following, we propose a model in order to evaluate the maximum achievable system throughput in downlink and to compare the performance of H-MFAP with those suggested and examined in the literature so far: L-MFAP with Non-orthogonal allocation scheme, L-MFAP with Orthogonal allocation scheme, vehicle Without MFAP.

For the LTE downlink data transmissions, the base station selects a

Modulation	Code Rate	SINR (dB)	IM (dB)	SINR+IM (dB)
QPSK (2 bit/symbol)	1/8	-5.1	2.5	-2.6
	1/5	-2.9		-0.4
	1/4	-1.7		0.8
	1/3	-1		1.5
	1/2	2		4.5
	2/3	4.3		6.8
	3/4	5.5		8.0
	4/5	6.2		8.7
16QAM (4 bit/symbol)	1/2	7.9	3	10.9
	2/3	11.3		14.3
	3/4	12.2		15.2
	4/5	12.8		15.8
64QAM (6 bit/symbol)	2/3	15.3	4	19.3
	3/4	17.5		21.5
	4/5	18.6		22.6

Table 7.1: *Dowlink SINR requirements for Lte*

Modulation and Code Scheme (MCS) based on Channel Quality Indicator provided by mobile user. LTE specifications define several MCSs that are used depending on the radio link conditions: a higher order modulation (more bits per modulated symbol) and a higher code rate can be used only when channel conditions are good, i.e. the SINR is sufficiently high. In our simulations we adopt the parameters of SINR requirements vs. MCS (see Table 7.1) presented in [46]. Please note that, as suggested in [46], we use an extra Implementation Margin (IM) for the difference in SINR requirements between theory and practical implementation.

The minimum LTE radio resource allocated to user is a Resource Block which consists of 12 subcarrier (180 KHz) assigned for 0.5 ms.

We consider a LTE frame structure with normal cyclic prefix with 7 OFDM symbol per subcarrier, so there are 84 symbols per Resource Block (RB). By applying the data of Table 7.1, for each SINR value we can calculate the amount of bits in each RB, Q as:

$$Q(SINR) = \frac{x\ bit}{symbol} \cdot code\ rate \cdot 84\ [bit/RB] \tag{7.18}$$

At the sole aim of comparing the several MFAP solutions, we can assume a fair allocation of resources to N_{UE} greedy users (sum of all $VUEs$, N_{VUE}, and out_UEs, N_{out_UE}) and we evaluate the achievable maximum system throughput.

To calculate the system throughput, we consider a Transmission Time Interval (TTI) of 1 ms. Notice that, in a system with MFAPs, the transmission in the backhaul link and access link occurs in two different intervals. For simplicity, we consider that the transmissions take place in the first and the second slots of the same TTI, respectively. Finally, it is necessary to observe that the amount of bits that a MFAP can send to $VUEs$ in the access link is limited by the number of bits that the eNodeB has previously sent to the MFAP in the backhaul link. For each link and solution considered, the SINR value is calculated using the formulas (7.6), (7.7), (7.8), (7.9), (7.10), (7.12), (7.14), (7.15), (7.16). So, the maximum system throughput calculation, Th^x, for the moving network solution x (x=**W**, **O**, **N**, **H**), can be calculated as:

$$Th^x = \sum_{i=1}^{N_{out\_UE}} Th_{out\_UE,i} + \sum_{j=1}^{J} \sum_{k=1}^{N_{VUE,j}} Th_{VUE,jk} \tag{7.19}$$

where J is the number of MFAP considered and $N_{VUE,j}$ the number of VUEs located in the vehicle with the $MFAP_j$.

Based on previous assumptions and observations, we have derived the $Th_{out\_UE,i}$ and $Th_{VUE,jk}$ in the following formulas for all the cases considered.

7.3.1 Without MFAP

In a configuration without MFAP the terms of (7.19) are calculated as follows:

$$Th^{W}_{out\_UE,i} = \frac{N_{RB}}{N_{UE}} \left\{ \frac{Q(SINR^{W}_{D,i})}{0.5 \cdot 10^{-3}} \right\} \tag{7.20}$$

$$Th^{W}_{VUE,k} = \frac{N_{RB}}{N_{UE}} \left\{ \frac{Q(SINR^{W}_{e,k})}{0.5 \cdot 10^{-3}} \right\} \tag{7.21}$$

where N_{RB} is the total number of Resource Blocks for the considered LTE system bandwidth. To calculate (7.20) and (7.21), we have considered one time slot (0.5 ms) and that all RBs are fairly allocated to the N_{UE} users. Therefore, we have evaluated the amount of bits per RB sent to each user depending on relative SINR measured.

7.3.2 L-MFAP with Orthogonal allocation scheme

In the case of Pure LTE MFAP that uses an orthogonal allocation scheme, the throughput for the out_UEs and $VUEs$ is calulated as:

$$Th^{O}_{out\_UE,i} = \frac{N_{RB}}{N_{UE}} \left\{ \frac{2 \cdot Q(SINR^{O}_{D,i})}{10^{-3}} \right\} \tag{7.22}$$

$$Th^{O}_{VUE,jk} = \frac{N_{RB}}{N_{UE}} \left\{ \frac{min\left[Q(SINR_{B,j}), Q(SINR^{O}_{A,jk})\right]}{10^{-3}} \right\} \quad (7.23)$$

For deriving eq. (7.22), we have considered that for each RB bandwidth assigned to the out_UE_i, the eNodeB in 10^{-3} ms (two time slots) can transmit two different data blocks to out_UE_i. Instead in (7.23), the amount of bits received by each VUE_{jk} is the minimum between the amount of bits that its serving $MFAP_j$ has previously received in the backhaul link and those it could send in the access link.

7.3.3 L-MFAP with Non-orthogonal allocation scheme

By considering a Pure LTE MFAP with non-orthogonal allocation scheme, we calculate the users throughput as:

$$\begin{aligned} Th^{N}_{out\_UE,i} &= \frac{1}{10^{-3}} \left[\frac{N_{RB}}{N_{UE}} (Q(SINR^{N}_{D,i})) + \frac{N_{RB}}{N_{out\_UE}} (Q(SINR^{N}_{D,i})) \right] \\ &= \frac{N_{RB}(N_{out\_UE} + N_{UE})}{N_{UE} \cdot N_{out\_UE}} \cdot \frac{Q(SINR^{N}_{D,i})}{10^{-3}} \end{aligned} \quad (7.24)$$

$$Th^{N}_{VUE,jk} = \frac{1}{10^{-3}} \left\{ min \left[\frac{N_{RB}}{N_{UE}} Q(SINR_{B,j}), \frac{N_{RB}}{N_{VUE,j}} Q(SINR^{N}_{A,jk}) \right] \right\} \quad (7.25)$$

In this case, in the second time slot, each access point (eNodeB

and L-MFAP) disposes of the whole bandwidth (N_{RB}) that can fairly allocate to its connected UEs. So, in the access link, each L-MFAP has more RBs available for sending the amount of bits that it has received in the backhaul link in the previous time slot.

7.3.4 H-MFAP

In our proposed system, the H-MFAP, the throughput of out_UEs and $VUEs$ is calculated as:

$$Th^{H}_{out\_UE,i} = Th^{N}_{out\_UE,i} \tag{7.26}$$

$$Th^{H}_{VUE,jk} = min\left[\frac{N_{RB}}{N_{UE}} \cdot \frac{Q(SINR_{B,j})}{10^{-3}}, \frac{Th^{H}_{A}}{N_{VUE,j}}\right] \tag{7.27}$$

where Th^{H}_{A} is the total throughput in the mmWave access link shared by VUEs connected to the $H - MFAP_j$. The throughput calculation for H-MFAP solution is analogous to that for L-MFAP with non-orthogonal allocation scheme, except, obviously, for the access link. Please note that the mmWave radio access has not yet been standardised. However, some studies presented in literature [24, 25, 42] provide the achievable throughput values in function of the SINR measured by the UE.

CHAPTER

EIGHT

CASE STUDIES AND SIMULATION RESULTS

In this section we present the results of our analysis. We compare the performance of our MFAP solution, H-MFAP, with other solutions proposed in literature, by means of Matlab simulations. The system parameters are shown in Table 8.1.

8.1 Scenario "Sub-urban"

We consider a single bus equipped with a MFAP that moves with constant velocity in a macrocell area. The bus starts its route near the eNodeB, then moving away, accosts to a greedy out_UE, located at 100 meters from the eNodeB. Inside the bus there is a single greedy VUE distant 5 m from the MFAP. Both eNodeB and MFAP transmit with constant power per Resource Block. Firstly, we focus on SINR measured by the VUE. Fig. 8.1 shows the SINR levels measured in the backhaul and access links. When the vehicle is more than 200 m from

the eNodeB, any solution with MFAP exhibits higher values of $SINR_A$ than those without MFAP, $SINR_e^W$. These results reinforce the need to use Moving Networks. However, not all MFAP schemes ensure high performance in a realistic and dynamic scenario. In fact, while the performances of L-MFAP with Orthogonal scheme and H-MFAP are constant, the $SINR_A^N$ degrades significantly when the bus is near the eNodeB site. This is because the eNodeB signal strength is too high and the metal walls of the bus are not able to insulate the vehicle. Only if the MFAP moves far away from the eNodeB, the interference on access links due to the direct link transmissions becomes negligible. Also, Fig. 8.1 shows that the constant $SINR_A^H$ value is almost always less than $SINR_A^N$ and $SINR_A^O$ values, but its value is high enough for not limiting the maximum achievable throughput. In fact, in our simulation the value of $SINR_A^H$ equals 22.64 dB, that is more than 21 dB, enough for a VUE to obtain a data rate of 990 Mbps, as proved in [24]. This value is considerably higher than the maximum throughput achievable in LTE-based backhaul link. So, the calculation of Th_{VUE} in eq. (7.27) depends only on the backhaul link throughput.

In fig. 8.2 we show the $SINR_D$ values measured when the single out_UE is at 100, 400, or 600 meters away from the eNodeB and the minimum distance from the MFAP is 10 meters in any case considered. Obviously the proximity of vehicle equipped with H-MFAP or L-MFAP with orthogonal allocation scheme does not affect the constant $SINR_D$ value measured by out_UE. Instead the proximity of L-MFAP with non-orthogonal scheme always results significant. The $SINR_D^N$ value notably decreases when the bus passes near the out_UE. This is because the LTE antenna inside the bus cannot have high directivity and, consequently, the signal strength is sufficiently high to

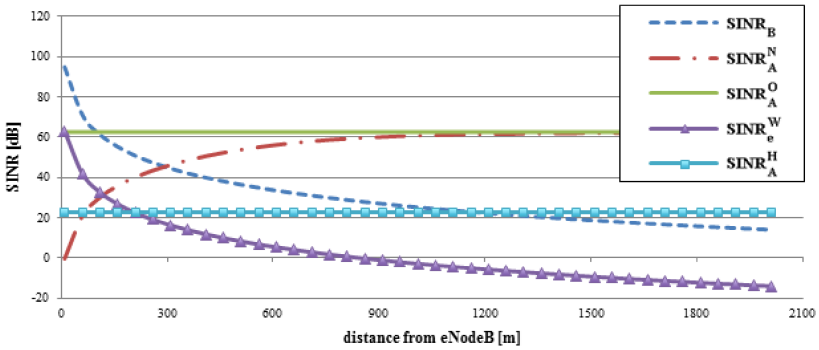

Figure 8.1: *SINR in dB measured in backhaul (dotted line) and access link in different configuration of MFAP: non-orthogonal scheme (line with dots and dashes), orthogonal scheme (solid line), in a configuration without MFAP (line with triangles) and with H-MFAP (line with square).*

cross the metal walls and interfere with the direct links.

In Figure 8.3, we compare the measurements of the maximum achievable throughput by the entire system for each solution, using the formulas (7.19), (7.20), (7.21), (7.22), (7.23), (7.24), (7.25), (7.26), (7.27), derived in our analysis. When the vehicle without MFAP moves away from the eNodeB, the throughput rapidly decreases already by 300 meters of distance. This is because the eNodeB signal reaches the VUE too weak ($Th_{VUE} \rightarrow 0$) and only the *out_UE* can exploit the resources of him allocated, so the total throughput reaches only 50% of maximum capacity. In the case of L-MFAP with orthogonal allocation scheme, the system is able to guarantee a throughput to VUE up to 1200 m, but with a waste of 25% of resources that increases with the increasing of the number of MFAPs. It represents a high price to

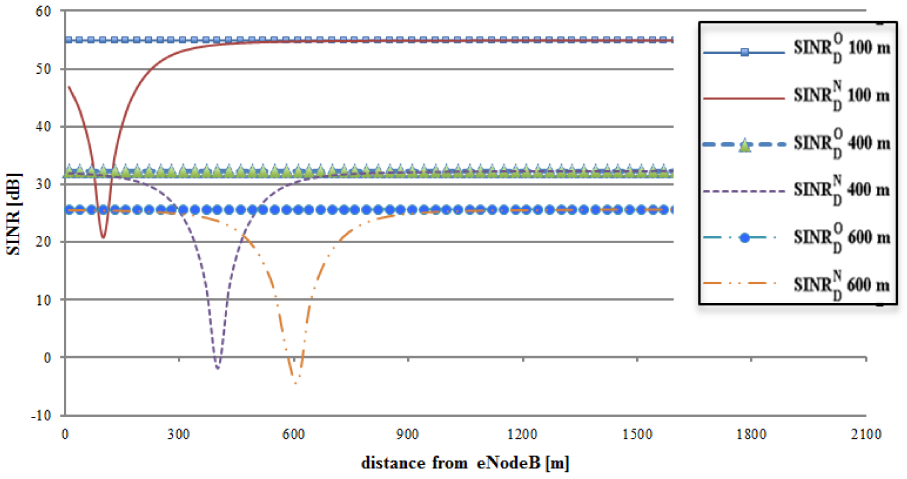

Figure 8.2: *SINR measured in the direct link vs different out_UE positions by benchmarking the L-MFAP with orthogonal and non-orthogonal allocation scheme*

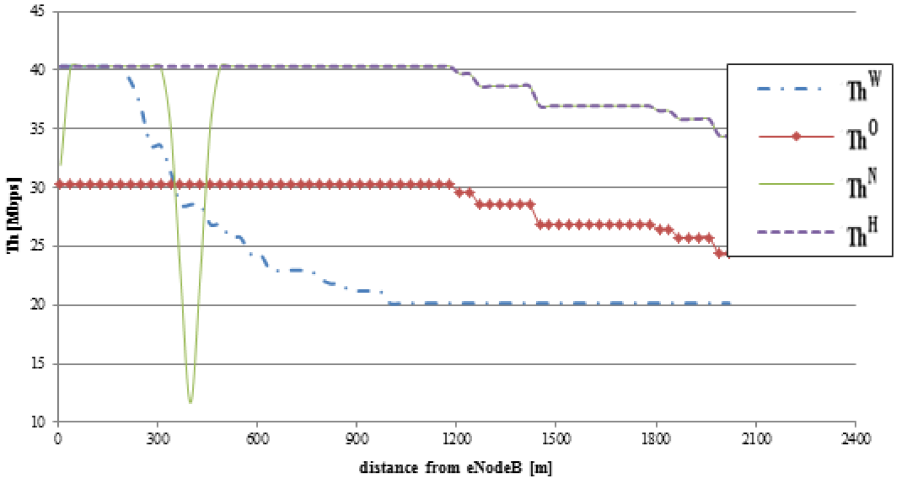

Figure 8.3: *Overall system Throughput in a scenario without MFAP (line with dots and dashes), with L-MFAP with orthogonal allocation scheme (line with triangles), with non-orthogonal allocation scheme (solid line), and with H-MFAP (dashed line)*

pay in contrast with one of the 5G requirements that is the increase of the spectral efficiency. In the case L-MFAP with non-orthogonal allocation scheme, the system can work at its full capacity, but under specific restrictions: the MFAP must move away from eNodeB and out_UEs. In fact, the performance degrades significantly when the vehicle is close to eNodeB (Th_{VUE} is almost zero up to 50 meters) and when the vehicle passes near an out_UE that causing a drastic reduction of Th_{out_UE}.

Finally, the H-MFAP outperforms both L-MFAP allocation schemes. In fact, the H-MFAP presents an overall increase in throughput of 33% compared to the orthogonal scheme and it does not suffer from severe limitations to its proximity to the eNodeB and out_UEs, as shown in L-MFAP with non-orthogonal allocation scheme.

Please note that, when the vehicle exceeds 1200 meters of distance from eNodeB, the total throughput degrades with any investigated solutions. This is because, despite the additional gain of the external MFAP antenna, the $SINR_B$ decreases under the values of 22.6 dB, i.e. the minimum requirement to apply the MCS that ensures the highest throughput (see Table 7.1). As a result, from this distance onwards, the Th_B represents an upper bound for the Th_{VUE}.

8.1.1 Multi-MFAPs configuration

The robustness of our proposal is evaluated by examining whether and how the presence of two nearby vehicles equipped with MFAPs (Multi-MFAPs) can affect the performance of the system.

At first sight, we evaluate the SINR measured by an out_UE and a VUE by using the equations (7.10), (7.12), (7.14), (7.15). Firstly we

analyse a single MFAP deployed in a bus that moves with a constant velocity in a macrocell area. Then we consider two buses distant 10 meters apart, with a MFAP for each one. For each scenario, there is an out_UE located at 500 meters from the eNodeB and a VUE distant 5 m from its serving MFAP. Each simulation is repeated by considering a configuration with L-MFAP in Non-orthogonal allocation scheme and one with H-MFAP.

Comparing the curves of Access and Direct Links in a configuration with L-MFAP with 1 and 2 vehicles, both UEs are influenced by the transmissions of neighbouring MFAP. In fact, in these links, the SINR measured in the scenario with two L-MFAPs is lower than the SINR with one bus (see $SINR_A^N$ and $SINR_D^N$ with one and two buses in fig. 8.4). This is because the metal walls of the bus do not perfect insulate the transmissions of the MFAP to the outside.

In our proposal, the features of frequencies at 60 GHz and the metal structure of the bus, perfectly isolate the two buses, such as to clear the inter-MFAPs interference (see $SINR_A^H$ with 1 and 2 buses in fig. 8.4). Moreover, when we use the mmWave in Access Link, the users of the direct link keep unchanged their SINR, because they are not affected by the presence of the bus as they work in the LTE frequencies (see $SINR_D^H$ in fig. 8.4).

After evaluating the SINR, we estimate the maximum capacity per Resource Block achievable by using the Shannon formula:

$$C = B \cdot log_2(1 + SINR) \tag{8.1}$$

where B is the bandwidth of a Resource Block (180 KHz) in LTE. For the mmWave, we consider a transmit unit that has a bandwidth

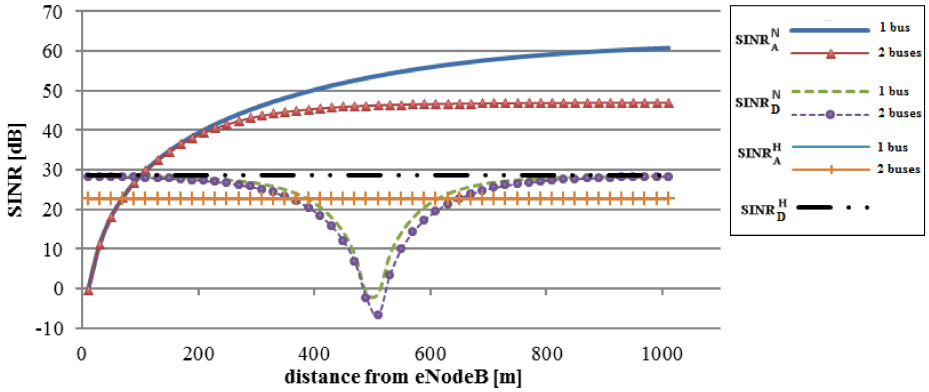

Figure 8.4: *$SINR_A^N$, $SINR_D^N$, $SINR_A^H$, $SINR_D^H$ with 1 or 2 MFAPs in a configuration with L-MFAP in non-orthogonal allocation scheme and H-MFAPs.*

proportional to the LTE one. So, for a carrier of 60 GHz, a mmWave-RB has a bandwidth of 4.15 MHz [22].

It is necessary to consider that the capacity of the access link for a VUE is limited by the capacity of the backhaul link. For this reason it is calculated as follows:

$$C_{VUE} = min(C_A, C_B) \tag{8.2}$$

where C_A is the access link capacity calculated both in LTE and in mmWave technology by using the $SINR_A^N$ (7.12) and $SINR_A^H$ (7.15) respectively, and C_B is the backhaul link capacity by using SINR calculated with eq. (7.6).

For an out_UE, the direct link capacity is calculated as follows:

$$C_{out\_UE} = C_D \tag{8.3}$$

where C_D is the direct link capacity calculated by using equations (7.10) and (7.14) in the cases of L-MFAP with non ortoghonal allocation scheme and H-MFAP respectively.

Moreover, also the capacity of a vehicular user in a configuration without MFAP is evaluated and calculated by using the following formula:

$$C_e^W = B \cdot log_2(1 + SINR_e^W) \tag{8.4}$$

where $SINR_e^W$ is calculated by using eq. (7.7).

In fig. 8.5 are shown the simulation results obtained in a configuration with two buses equipped with MFAP. The capacity per RB for a VUE in a configuration without MFAP (C_e^W) decreases when it moves away from the serving eNodeB. The presence of two nearby L-MFAP in non-orthogonal allocation scheme causes a decrease of the capacity for the $VUEs$, when the buses are near the eNodeB, due for the transmission of the direct link, and for the out_UE when the L-MAPs are near to it. In the same conditions, the higher bandwidth of the access links in mmWave allows $VUEs$ of a H-MFAP to have a high capacity, especially when the buses are close to the eNodeB. Moreover, the capacity of the out_UE remains unchanged because different frequency bands are used inside and outside the H-MFAP. Notice that, from 300 m onwards, the backhaul link limits the capacity of the access links in both L-MFAP and H-MFAP configurations.

Finally, the inter-MFAP interference effect is evaluated in term of throughput by applying the equations (7.24), (7.25), (7.26), (7.27) in a configuration with two nearby L-MAPs with non-orthogonal allocation scheme and with two H-MFAPs.

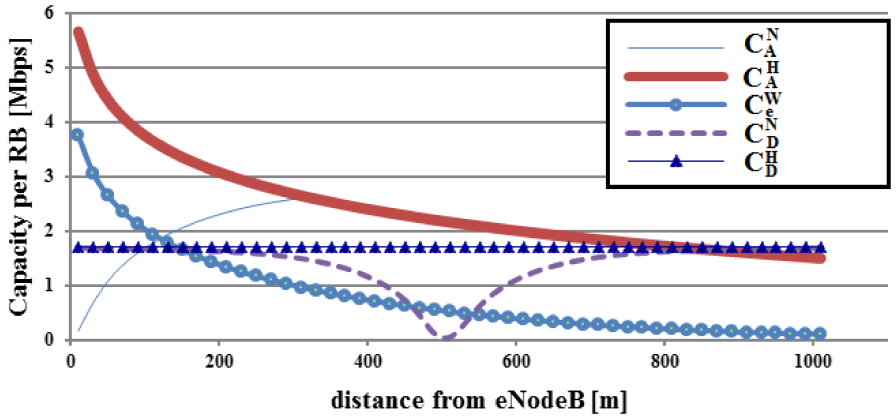

Figure 8.5: *Comparison of the capacity per Resource Block in a configuration with two L-MFAPs and two H-MFAP.The capacity of a VUE is displayed with a solid line in the case of two nearby H-MFAP, and with a thin line in a configuration with two nearby L-MFAP. The out_UE's capacity is shown with dashed line for the simulations with two L-MFAPs, while a line with triangles is used for displaying the same parameter with H-MFAPs.A line with circles shows the capacity for a VUE in a vehicle without MFAP.*

The simulation results show that, although the $SINR_A^N$ decreases when two bus with L-MFAPs are near (see fig. 8.4), the transmitting power of the MFAP is so high as to counteract the effect of interference of neighboring L-MFAP. So, in no case investigated it has been measured a significant inter-MFAP interference that can alter the throughput performances for VUEs. Instead, in the only case of L-MFAP with non-orthogonal scheme, the *out_UE* throughput is further degraded by the presence of two nearby L-MFAPs. For example, when a greedy *out_UE* is located at 100 meters from the eNodeB and 10 meters from a L-MFAP, the system throughput is 35.28 Mbps and decreases until 30.24 Mbps if another vehicle equipped with L-MFAP approaches, as shown in Fig. 8.6.

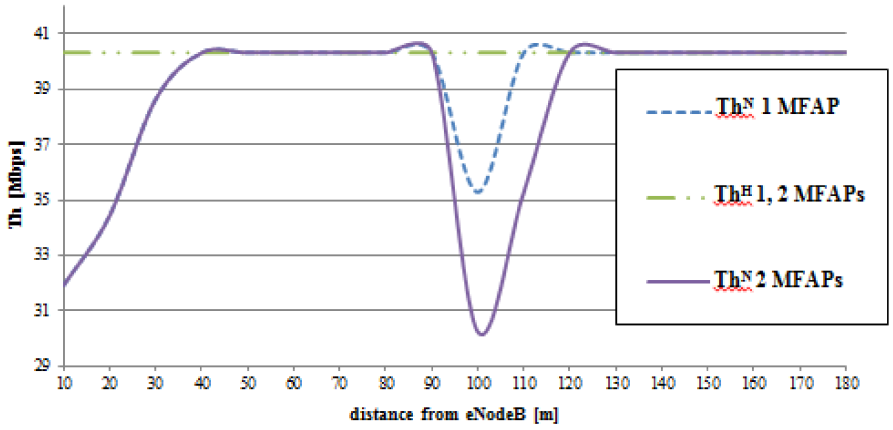

Figure 8.6: *System throughput with 1 or 2 MFAPs in a configuration with L-MFAP in non-orthogonal allocation scheme with a vehicle (dashed line) and two vehicles (solid line). The line with dots and dashes shows the system Throughput in a scenario with 1 or 2 H-MFAPs.*

8.2 Scenario "Urban"

In the previous sub-section, we have seen the better performance of L-MFAPs in non-orthogonal allocation scheme than those that work in orthogonal scheme. For this reason, in the following, we only consider L-MFAP with non-orthogonal allocation scheme.

Firstly we examine the VUE performance when a vehicle equipped with a L-MFAP moves in a picocell area at different distance d from the pico base station. We want to evaluate the inter-cell interference between a VUE and a $pico\_UE$ that use the same RB assigned by own serving base station.

The $SINR_A$ measured by a VUE is shown in Fig. 8.7. As we expected, the $SINR_A$ decreases when the L-MFAP is near to a pico base stations, however, thanks to the insulating effect of the VPL and the lower transmitting power of a pico base station than those of a eNodeB, its value is high enough (58.6 dB) to achieve the maximum bit rate in according to MCS (see Table 7.1). Moreover, as already seen in "sub-urban" scenario, the presence of two nearby MFAPs does not affect the performance of the VUEs in both cases of L-MFAP and H-MFAP. Due to these results, we focus only on the performance of the $pico\_UE$ in the three following case studies.

Firstly, by using (7.16), we evaluated the SINR of a $pico\_UE$, by varying two parameters: the distance between the $pico\_UE$ and its serving cell ($D_p \in [5, 100]\ m$), and the distance between the $pico\_UE$ and the L-MFAP ($d_{M-FAP} \in [2, 50]\ m$). The simulation results reported in Fig. 8.8 show a very wide variation of $SINR_{pico\_UE}$ values. More specifically, Fig 8.9 shows the couple of values of D_p and d_{M-FAP} when the SINR of the $pico\_UE$ reaches the minimum ad-

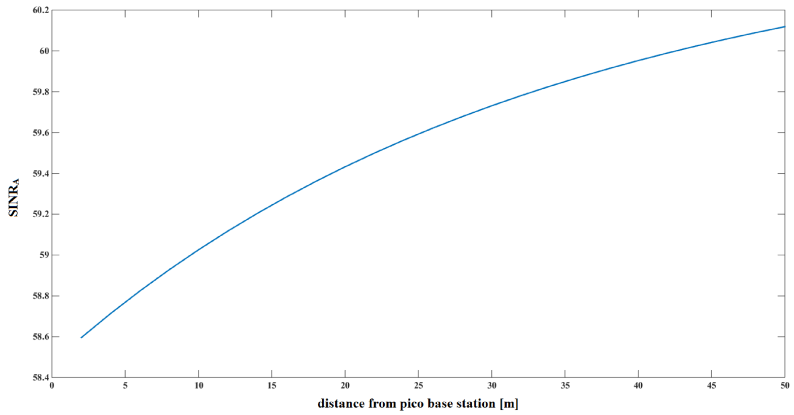

Figure 8.7: *$SINR_A$ measured by a VUE vs distance from the pico base station*

missible value for each type of modulation, e.g. SINR={-2.6, 10.9, 19.13} dB (see Table 7.1). Let's note that in the region when the $SINR_{pico\_UE} < -2.6\,dB$, the connections are dropped, in fact, in this case, the UE can't demodulate the signal in according to Table 7.1, and it may occur even in cases where the *pico_UE* is not so far away from serving picocell ($D_p > 10\,m$).

In order to evaluate the total throughput of a picocell crossed by a bus equipped with a L-MFAP, we have considered a second urban setup. We perform a series of Matlab simulations in which there are N greedy *pico_UEs* randomly placed with an uniform distribution in a picocell area with a radius of 100 mt and a bus crosses the picocell with constant velocity v=20 m/s and with a random distance from the pico base station. We assume that the resources are fairly allocated by the pico base station to the *pico_UEs* (N_{RB}/N Resource Blocks for

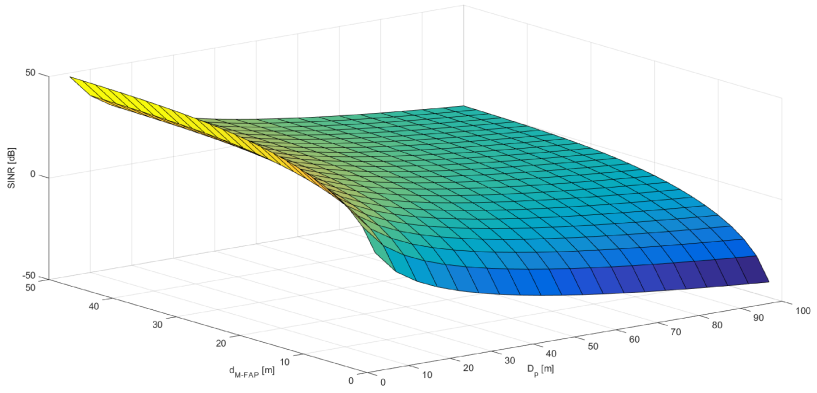

Figure 8.8: *$SINR_{pico\_UE}$ vs d_{M-FAP} and D_p*

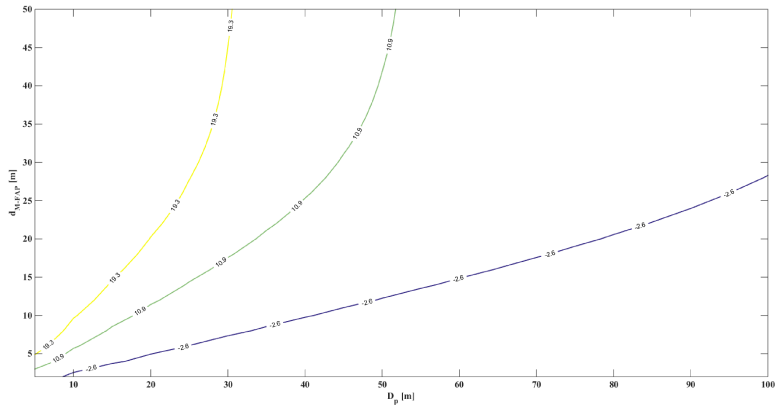

Figure 8.9: *Values of D_p and d_{M-FAP} for SINR={-2.6,10.9,19.3} dB*

each $pico\_UE$). So, we calculate the instantaneous picocell as follows:

$$Th_{pico} = \sum_{i=1}^{N} \frac{N_{RB}}{N} \cdot \frac{Q(SINR_{pico\_UE,i})}{0.5 \cdot 10^{-3}} \, [bps] \tag{8.5}$$

where $Q(SINR_{pico\_UE,i})$ is calculated by using (7.18) with the SINR measured using (7.16). Furthermore we compare this value with the one obtained in the same scenario but using a H-MFAP solution. Fig 8.10 shows the cdf of the average Th_{pico} values calculated with N=10 greedy $pico\_UEs$. We can see how the presence of the L-MFAP heavily degrades the throughput of the picocell.

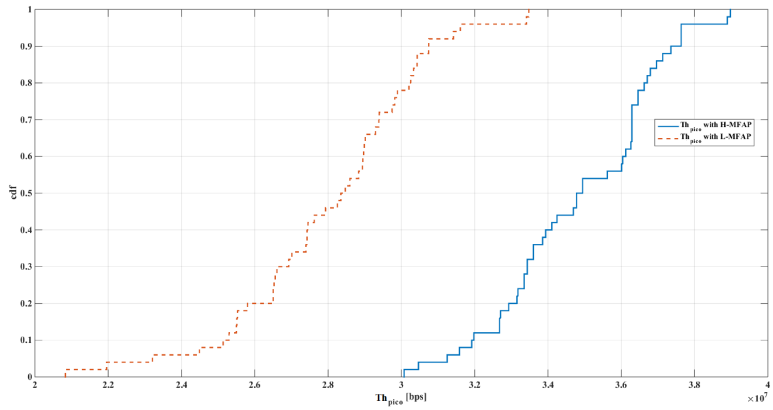

Figure 8.10: *Average picocell throughput (Th_{pico}) in bps for 10 $pico\_UE$. The solid line is the Th_{pico} measured in a scenario with a H-MFAP. The dotted line is the Th_{pico} in the same scenario but with the presence of a vehicle equipped with a L-MFAP*

For each simulation (same positions of the $pico\_UEs$ and same bus route), we also calculate the Throughput Gain with H-MFAP vs

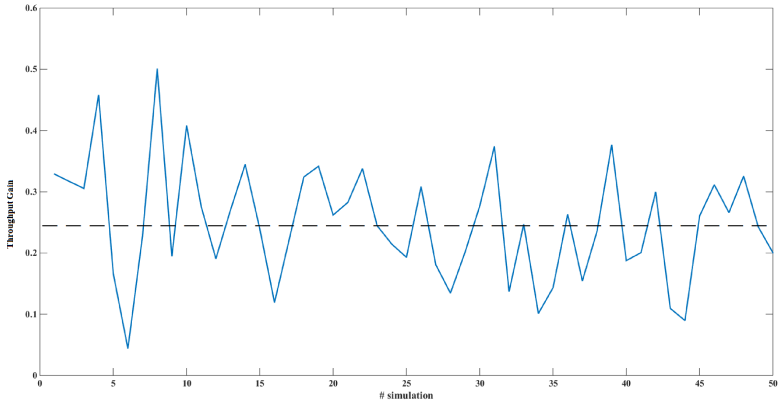

Figure 8.11: *Throughput Gain (solid line), average Throughput Gain (dashed line) on 50 simulations*

L-MFAP (see Fig. 8.11). The results demonstrate that the use of a H-MFAP makes the throughput of a picocell increased with an average of 24.88% with a standard deviation of 9.43%.

However, in Fig. 8.11 we can also note that the gain varies from about 5% to 50%. This is due to the random position of the bus respect the location of the pico base station. Based on this observation, we wonder if in a realistic scenario will yet reached such a high gain value as to maintain high the throughput value. For this reason, in the following, we want to examine a third configuration, a typical urban setup proposed in Metis [47] and used by researchers in [5].

We simulate a simplified Madrid grid model with a heterogeneous deployment of macrocell, picocells, and L-MFAPs. In particular we consider a macro cell area with an eNodeB that transmits at 800 MHz where there are buildings of 120by120 meters surrounded by streets

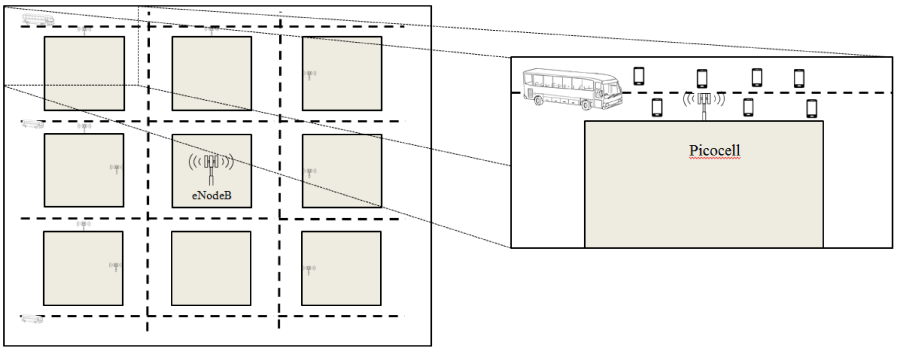

Figure 8.12: *Focus of Madrid grid model with a heterogeneous deployment of macrocell, picocells and vehicles equipped with MFAP*

of 21 meters. The coverage of the streets is enhanced by the presence of LTE picocells, deployed as shown in Fig. 8.12. Both picocells and L-MFAPs work in the same LTE bandwidth, so there will be an interference between the transmissions of these two kind of small cells.

We analyse a focus of the model by considering a group of 10 $pico\_UEs$ deployed along a street covered by the picocell. The positions of the $pico\_UEs$ are random with an uniform distribution. A bus equipped with L-MFAP across the street with a random route. Due to the small width of the streets, the density of the $pico\_UEs$ is higher and the L-MFAP is closer to them than the second configuration of Scenario “Urban”. We perform a series of simulations by varying the positions of the $pico\_UEs$ and the buses. For each simulation we collect the throughput of the picocell by using (8.5), and, with the same conditions, we replaced the L-MFAP with H-FAP. Finally, we calculate the cdf of the total average throughput of the picocell.

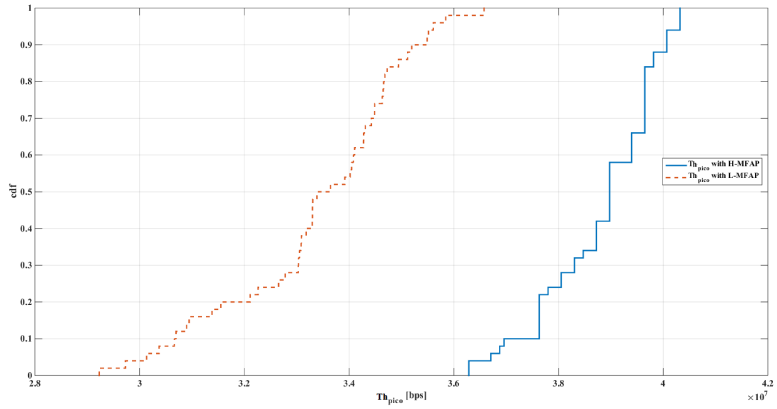

Figure 8.13: *Cdf of Th_{pico} in bps. The solid line is the Th_{pico} measured in a scenario with a bus with a H-MFAP. The dotted line is the Th_{pico} in the same scenario with the presence of a vehicle equipped with a L-MFAP*

The results are shown in Fig. 8.13. As in the second configuration of Scenario "Urban", the use of the H-MFAP in the bus increases the performance of the system. We calculated a Throughput Gain of 38.96% with a standard deviation of 7.84%.

Parameter	**Symbol**	**Value**
LTE bandwith		10 MHz
mmWave bandwith		220 MHz
Transmit Power of eNodeB	P_1	46 dBm
Transmit Power of MFAP	P_2	23 dBm
Transmit Power of Picocell	P_3	23 dBm
Speed buses	v	20 m/s
Wall Penetration Los in LTE	Lw_1	20 dB
Wall Penetration Los in mmWave	Lw_2	40.1 dB
MFAP Antenna Gain	Ag	8 dB
Noise Figure in LTE	NF_1	5 dB
Noise Figure in mmWave	NF_2	8 dB
Shadowing Standard Deviation for SMa	σ_1	6 dB
Shadowing Standard Deviation for InH	σ_2	3 dB
Shadowing Standard Deviation for mmWave	σ_3	0.88 dB
Shadowing Standard Deviation for UMi	σ_4	7 dB

Table 8.1: *System Parameters*

CHAPTER

NINE

CONCLUSIONS

In the thesis we have introduced the concept of Hybrid-Mobile Femtocell, combining LTE and mmWave technologies, as a new proposal for the Moving Networks.

We have shown that the mmWave is a ready and suited technology to be applied in vehicular environments, so we analysed the feasibility of our proposal in two different system configuration that can be adopted in sub-urban and urban scenarios. In the first, L-MFAPs and eNodeB use the same frequency band, while in the latter, we consider that macrocells and small cells work in different LTE frequencies in order to eliminate the cross-layer interference. In particular we propose a scenario where eNodeB transmits at 800 MHZ, while both picocells and L-MFAP work at 2.6 GHz.

In order to compare H-MFAP performance with other L-MFAP solutions presented in literature, we have introduced a new throughput analysis, assuming the presence of greedy users and a fair allocation

of RB to them. The simulation results in a "sub-urban" scenario show that the L-MFAP with orthogonal resource allocation scheme always guarantees a constant throughput to the VUEs, but with a waste of 25% of the resources with a single vehicle. The L-MFAP with non-orthogonal scheme, instead, achieves higher performance compared to that with the orthogonal scheme, but it suffers from the interference due to simultaneous transmission of the direct and access links. In particular we have noted the throughput of the VUE decreases when the bus is close to the eNodeB and the out_UE suffers from the presence of the L-MFAP when it is closed to him.

We have also evaluated when there are two neighbouring vehicles equipped with MFAP. It has not been measured a significant inter-MFAP interference that can alter the throughput for the VUEs in both scenarios with two L-MFAP and two H-MFAP thanks to the double insulating effect of the VPL. However, the proximity of two L-MFAPs with non-orthogonal allocation scheme greatly worsens the throughput of the out_UE, while the performance of this user remain unchanged when one or more H-MFAPs are near to it. This is an important result that provides the characteristics of scalability and robustness to our proposal.

So, in a "sub-urban" scenario, our proposal outperforms L-MFAP with both allocation schemes. In fact, the H-MFAP always presents an increase in overall throughput of 33% compared to the L-MFAP operating in orthogonal allocation mode, and it does not suffer from the drastic reduction in throughput that L-MAF with non-orthogonal allocation scheme exhibits when the vehicle is close to the eNodeB and/or an out_UE.

We have extended our analysis in an "Urban" topology where dif-

ferent kind of small cells can be deployed. In this case, we have analysed the performance of the $pico\_UEs$ connected to a picocell that transmits in the same LTE band of the L-MFAP. Once again, in several case studies, the L-MFAP with non-orthogonal allocation scheme heavily decreases the throughput of the $pico\_UEs$ located along its route. For example, we have evaluated that in a simplified Madrid grid model, the use of H-MFAP improves the performance of the $pico\_UEs$, obtaining a gain of about 39% than the solution with L-MFAP as suggested in literature.

In conclusion, in both sub-urban and urban deployment, the use of H-MFAPs guarantees high throughput to vehicular, macro, and pico users in any position where a vehicle can be, without excessive handover procedures and without waste of resources. So we believe that H-MFAP can be a potential candidate for the Moving Network in 5G era.

9.1 Future Works

The mmWave is a key element of the 5G network that meets the requirements of high availability, capacity, and elevate bit rates.

In this thesis, the integration of mmWave in a Moving Network architecture based on Mobile Femtocell Access Point, presents good results in terms of SINR and throughput to both vehicular users and macrocell and/or picocell users.

When the standardisation of mmWave as one of the 5G radio access will be ready, it is necessary to complete this work by using the physical and MAC layers that the technology will use. Moreover, to

meet the energy saving requirements of the new mobile network, it will be necessary to measure and compare the power consumption of the user equipment both in LTE and mmWave technology.

BIBLIOGRAPHY

[1] I. Hwang, B. Song, and S. S. Soliman, "A holistic view on hyper-dense heterogeneous and small cell networks," *IEEE Communications Magazine*, vol. 51, pp. 20–27, June 2013.

[2] Nokia Siemens Network, "2020: Beyond 4g: Radio evolutionfor the gigabit experience," white paper, Nokia Siemens Network, 2011.

[3] Cisco, "Cisco visual networking index: Global mobile data traffic forecast update, 2015-2020," white paper, Cisco, 2015.

[4] Qualcomm Incorporated, "The 1000x data challenge." `http://www.qualcomm.com/1000x/`, June 2013.

[5] Y. Sui, I. Guvenc, and T. Svensson, "Interference management for moving networks in ultra-dense urban scenarios," *EURASIP Journal on Wireless Communications and Networking*, vol. 2015, no. 1, pp. 1–32, 2015.

[6] A. Osseiran, F. Boccardi, V. Braun, K. Kusume, P. Marsch, M. Maternia, O. Queseth, M. Schellmann, H. Schotten, H. Taoka, H. Tullberg, M. A. Uusitalo, B. Timus, and M. Fallgren, "Scenarios for 5g mobile and wireless communications: the vision of the metis project," *IEEE Communications Magazine*, vol. 52, pp. 26–35, May 2014.

[7] Ericsson, "More than 50 billion connected devices," white paper, Ericsson, February 2011.

[8] M. ICT, "317669-metis/d1. 1,scenarios, requirements and kpis for 5g mobile and wireless system," 2013.

[9] P. Popovski, V. Braun, G. Mange, P. Fertl, D. Gozalvez-Serrano, N. Bayer, H. Droste, A. Roos, G. Zimmerman, M. Fallgren, *et al.*, "Initial report on horizontal topics, first results and 5g system concept," *METIS Deliverable D*, vol. 6, p. 2, 2014.

[10] T. E. Bogale and L. B. Le, "Massive mimo and millimeter wave for 5g wireless hetnet: Potentials and challenges," *arXiv preprint arXiv:1510.06359*, 10 2015.

[11] Huawei, "5g: A technology vision," white paper, Huawei, February 2014.

[12] C. X. Wang, F. Haider, X. Gao, X. H. You, Y. Yang, D. Yuan, H. M. Aggoune, H. Haas, S. Fletcher, and E. Hepsaydir, "Cellular architecture and key technologies for 5g wireless communication networks," *IEEE Communications Magazine*, vol. 52, pp. 122–130, February 2014.

[13] S. Jangsher and V. O. K. Li, "Resource allocation in cellular networks employing mobile femtocells with deterministic mobility," in *2013 IEEE Wireless Communications and Networking Conference (WCNC)*, pp. 819–824, April 2013.

[14] E. Tanghe, W. Joseph, L. Verloock, and L. Martens, "Evaluation of vehicle penetration loss at wireless communication frequencies," *IEEE TRANSACTIONS ON VEHICULAR TECHNOLOGY*, vol. 57, no. 4, pp. 2036–2041, 2008.

[15] J. G. Andrews, H. Claussen, M. Dohler, S. Rangan, and M. C. Reed, "Femtocells: Past, present, and future," *IEEE Journal on Selected Areas in Communications*, vol. 30, pp. 497–508, April 2012.

[16] A. Dudnikova, D. Panno, and A. Mastrosimone, "Measurement-based coverage function for green femtocell networks," *Computer Networks*, vol. 83, pp. 45 – 58, 2015.

[17] V. Chandrasekhar, J. G. Andrews, and A. Gatherer, "Femtocell networks: a survey," *IEEE Communications Magazine*, vol. 46, pp. 59–67, September 2008.

[18] F. Haider, C. X. Wang, H. Haas, D. Yuan, H. Wang, X. Gao, X.-H. You, and E. Hepsaydir, "Spectral efficiency analysis of mobile femtocell based cellular systems," in *Communication Technology (ICCT), 2011 IEEE 13th International Conference on*, pp. 347–351, Sept 2011.

[19] Y. Chen and X. Lagrange, "Downlink capacity gain analysis of mobile relay in lte-advanced network," in *2014 IEEE 11th Con-*

sumer Communications and Networking Conference (CCNC), pp. 544–550, Jan 2014.

[20] M. Z. Chowdhury, S. Q. Lee, B. H. Ru, N. Park, and Y. M. Jang, "Service quality improvement of mobile users in vehicular environment by mobile femtocell network deployment," in *ICTC 2011*, pp. 194–198, Sept 2011.

[21] Y. Sui, J. Vihriala, A. Papadogiannis, M. Sternad, W. Yang, and T. Svensson, "Moving cells: a promising solution to boost performance for vehicular users," *IEEE Communications Magazine*, vol. 51, pp. 62–68, June 2013.

[22] A. Mastrosimone and D. Panno, "New challenge: Moving network based on mmwave technology for 5g era," in *Computer, Information and Telecommunication Systems (CITS), 2015 International Conference on*, pp. 1–5, July 2015.

[23] A. Mastrosimone and D. Panno, "A comparative analysis of mmwave vs lte technology for 5g moving networks," in *Wireless and Mobile Computing, Networking and Communications (WiMob), 2015 IEEE 11th International Conference on*, pp. 422–429, Oct 2015.

[24] C. Dehos, J. L. González, A. D. Domenico, D. Kténas, and L. Dussopt, "Millimeter-wave access and backhauling: the solution to the exponential data traffic increase in 5g mobile communications systems?," *IEEE Communications Magazine*, vol. 52, pp. 88–95, September 2014.

[25] Z. Pi and F. Khan, "An introduction to millimeter-wave mobile broadband systems," *IEEE Communications Magazine*, vol. 49, pp. 101–107, June 2011.

[26] A. Damnjanovic, J. Montojo, Y. Wei, T. Ji, T. Luo, M. Vajapeyam, T. Yoo, O. Song, and D. Malladi, "A survey on 3gpp heterogeneous networks," *IEEE Wireless Communications*, vol. 18, pp. 10–21, June 2011.

[27] 3rd Generation Partnership Project, "3gpp tr 36.836 technical specification group radio access network; evolved universal terrestrial radio access (e-utra); study on mobile relay," tech. rep., 3rd Generation Partnership Project, June 2014.

[28] W. Li, C. Zhang, X. Duan, S. Jia, Y. Liu, and L. Zhang, "Performance evaluation and analysis on group mobility of mobile relay for lte advanced system," in *Vehicular Technology Conference (VTC Fall), 2012 IEEE*, pp. 1–5, Sept 2012.

[29] R. Raheem, A. Lasebae, M. Aiash, and J. Loo, "From fixed to mobile femtocells in lte systems: Issues and challenges," in *Second International Conference on Future Generation Communication Technologies (FGCT 2013)*, pp. 207–212, Nov 2013.

[30] R. Raheem, A. Lasebae, and J. Loo, "Performance evaluation of lte network via using fixed/mobile femtocells," in *Advanced Information Networking and Applications Workshops (WAINA), 2014 28th International Conference on*, pp. 255–260, May 2014.

[31] S. Chae, T. Nguyen, and Y. M. Jang, "A novel handover scheme in moving vehicular femtocell networks," in *2013 Fifth Interna-*

tional Conference on Ubiquitous and Future Networks (ICUFN), pp. 144–148, July 2013.

[32] M. Z. Chowdhury, S. H. Chae, and Y. M. Jang, "Group handover management in mobile femtocellular network deployment," in *2012 Fourth International Conference on Ubiquitous and Future Networks (ICUFN)*, pp. 162–165, July 2012.

[33] F. Haider, M. Dianati, and R. Tafazolli, "A simulation based study of mobile femtocell assisted lte networks," in *2011 7th International Wireless Communications and Mobile Computing Conference*, pp. 2198–2203, July 2011.

[34] IEEE, "Ieee 802.15.3c part 15.3: Wireless medium access control (mac) and physical layer (phy) specifications for high rate wireless personal area networks (wpans) amendment 2: Millimeter-wave-based alternative physical layer extension," tech. rep., IEEE, October 2009.

[35] IEEE, "Ieee 802.11ad. part 11: Wireless lan medium access control (mac) and physical layer (phy) specifications - amendment 3: Enhancements for very high throughput in the 60 ghz band," tech. rep., IEEE, December 2012.

[36] H. Shokri-Ghadikolaei, C. Fischione, G. Fodor, P. Popovski, and M. Zorzi, "Millimeter wave cellular networks: A mac layer perspective," *IEEE Transactions on Communications*, vol. 63, pp. 3437–3458, Oct 2015.

[37] E. Dahlman, G. Mildh, S. Parkvall, J. Peisa, J. Sachs, and Y. Selén, "5g radio access," *Ericsson review*, vol. 6, pp. 2–7, 2014.

[38] M. Willis, "An introduction to radiowave propagation, course notes." `http://www.mike-willis.com/Tutorial/PF5.htm`.

[39] R. J. Weiler, M. Peter, W. Keusgen, E. C. Strinati, A. De Domenico, I. Filippini, A. Capone, I. Siaud, A.-M. Ulmer-Moll, A. Maltsev, *et al.*, "Enabling 5g backhaul and access with millimeter-waves.," in *EuCNC*, pp. 1–5, 2014.

[40] F. Giannetti, M. Luise, and R. Reggiannini, "Mobile and personal communications in the 60 ghz band: A survey," *Wireless Personal Communications*, vol. 10, no. 2, pp. 207–243, 1999.

[41] K.-C. Huang and Z. Wang, *Millimeter wave communication systems*, vol. 29. John Wiley & Sons, 2011.

[42] T. Bai, A. Alkhateeb, and R. W. Heath, "Coverage and capacity of millimeter-wave cellular networks," *IEEE Communications Magazine*, vol. 52, pp. 70–77, September 2014.

[43] W. Hong, K. Baek, Y. G. Kim, Y. Lee, and B. Kim, "mmwave phased-array with hemispheric coverage for 5thgeneration cellular handsets," in *The 8th European Conference on Antennas and Propagation (EuCAP 2014)*, pp. 714–716, April 2014.

[44] 3GPP, "Technical specification group radio access network; evolved universal terrestrial radio access (e-utra); further advancements for e-utra physical layer aspects (rel. 9) tr 36.814 v.9.0.0," tech. rep., 3GPP, 2010.

[45] S. Geng, J. Kivinen, X. Zhao, and P. Vainikainen, "Millimeter-wave propagation channel characterization for short-range wire-

less communications," *IEEE Transactions on Vehicular Technology*, vol. 58, pp. 3–13, Jan 2009.

[46] M. Baker, S. Sesia, and I. Toufik, "Lte-the umts long term evolution from theory to practice," 2011.

[47] P. Agyapong, V. Braun, M. Fallgren, A. Gouraud, M. Hessler, S. Jeux, A. Klein, J. Lianghai, D. Martin-Sacristan, M. Maternia, *et al.*, "Ict-317669-metis/d6. 1 simulation guidelines," tech. rep., METIS Project, 2013.

LIST OF PUBLICATIONS

- A. Dudnikova, A. Mastrosimone, D. Panno, "Measurement-based coverage function for green femtocell networks", COMPUTER NETWORKS, ISSN: 1389-1286 (2015)
- A. Dudnikova, A. Mastrosimone, D. Panno, "A Measurement-Based Approach for Cognitive Femtocell Networks", Proc. European Wireless 2014, Barcelona, Spain, 14-16 May 2014.
- A. Dudnikova, A. Mastrosimone, D. Panno, "An adaptive pilot power control approach for green heterogeneous networks", Proc. 2014 European Conference on Networks and Communications (EuCNC), Bologna, Italy.
- A. Mastrosimone, D. Panno, "New Challenge: Moving Network based on mmWave Technology for 5G era", International Conference on Computer, Information and Telecommunication Systems 2015, Gijon, Spain
- A. Mastrosimone, D. Panno, "A comparative Analysis of mmWave vs LTE technology for 5G Moving Networks", The

11th IEEE International Conference on Wireless and Mobile Computing, Networking and Communications, Abu Dhabi (UEA), 19-21 October 2015.

- A. Mastrosimone, D. Panno, "Moving Network based on mmWave Technology: a promising solution for 5G Vehicular Users", Wireless Network, Springer (Under submission)